

A Geostatistical Approach to Denoise and Interpolate Experimental Complex-Valued B_1^- Maps

G. Ferrand¹, M. Luong¹, P. Chauvet², M. A. Cloos³, and A. Amadon³

¹IRFU/SACM, CEA Centre de Saclay, Gif sur Yvette, France, ²Centre de Géosciences, Mines ParisTech, Fontainebleau, France, ³DSV/I2BM/NeuroSpin/LMRN, CEA Centre de Saclay, Gif sur Yvette, France

INTRODUCTION The knowledge of the complex-valued B_1^- map generated by each channel of a phased-array RF coil has become essential for high field MRI systems operating above 7 T, a cornerstone for static or dynamic shimming techniques, whose aim is to provide a uniform excitation over any region of interest (ROI). The maps must be measured experimentally for each RF coil and each subject under examination using a specific MRI sequence, so-called AFI [1]; the more accurate and space resolved the maps, the higher the shimming quality. Unfortunately, high quality maps are time consuming and usually lead to a stronger SAR exposure for the subject. We propose in this abstract a new method based on geostatistical considerations to post-process noisy and poor space resolved B_1^- maps. A proof of principle experiment is reported for a homogeneous spherical phantom at 7 T.

METHOD The input data for the post-processing method are complex-valued B_1^- phase vector maps measured in the spin rotating frame, over a discrete 3D grid. The principle of the method is based on the assumption that a B_1^- distribution is not totally unpredictable, i.e. the difference between values measured at two positions close to each other is lower than the one measured at two faraway positions, due to the physical nature of the B_1^- distribution in the head. Besides, the post-processing uses the continuity property of the magnetic field because the permeability is the same everywhere. In this particular case, we are able to evaluate the magnetic field at new positions (interpolation) or to reevaluate it at measured positions (denoising) with 3D kriging technique [2]. In the first place, we consider the measured field as a random variable $B_{1m}^+(\vec{x})$ known for all the positions: $\vec{x}_1, \dots, \vec{x}_n$ where a measurement is made, and in the second place, we evaluate this random variable, for a new position \vec{x}_α , with $B_{1m}^+(\vec{x}_\alpha)$ unknown, using the kriging technique:

$$B_{1k}^+(\vec{x}_\alpha) = \sum_{i=1}^n \lambda_i(\vec{x}_\alpha) B_{1m}^+(\vec{x}_i) \text{ with } \sum_{i=1}^n \lambda_i(\vec{x}_\alpha) = 1$$

To minimize the variance of $B_{1k}^+(\vec{x}_\alpha) - B_{1m}^+(\vec{x}_\alpha)$, we use the variogram:

$$\gamma(h) = \frac{1}{2} \text{Var}(B_{1m}^+(\vec{x}_a) - B_{1m}^+(\vec{x}_b)), \text{ with } h = \|\vec{x}_a - \vec{x}_b\|.$$

Kriging allows to reevaluate the measured map $B_{1m,j}^+(\vec{x})$ for channel j , into a kriged map $B_{1k,j}^+(\vec{x})$ or to interpolate from $B_{1m,j}^+(\vec{x})$ to $B_{1m,j}^+(\vec{x} + \vec{\delta})$. Since $B_{1m,j}^+(\vec{x})$ is a complex value, we decided to krig separately the real part and the imaginary part. However, we have actually $B_{1m}^+(\vec{x}) = B_1^+(\vec{x})e^{i\varphi(\vec{x})}$, where $\varphi(\vec{x})$ is an unknown phase distribution related

to the image construction and not provided by the AFI sequence, which breaks the continuity property of B_1^- . One solution to recover this property could consist in dividing the measured maps by a reference map, which could be the map obtained from a well-chosen interference, and then multiplying by the amplitude map of the same reference. However, best results for each individual channel map are achieved while combining the most relevant information provided by several krigings with several reference maps.

RESULTS To test our technique, the maps were first measured with an AFI 3D sequence ($32 \times 32 \times 22$ resolution). The RF coil used in this study consisted of eight dipoles distributed in 40-degree increments in the azimuth coordinate, leaving an aperture for visual stimulation. A round bottom flask of 16 cm diameter, filled with a CuSO_4 -doped saline solution provided a spherical homogeneous phantom with a T_1 of 330 ms. The measurement of a map lasted 70 s for each channel. Figure 1 shows a noise reduction in the axial plane (xy) and a resolution improvement in the sagittal plane (xz , we defined x as vertical and y as horizontal) after a kriging in the z -direction with a resolution of $32 \times 32 \times 44$. Results are given here for one interference, instead of one channel map, to show the promising capabilities of this processing technique in the case of a more complex distribution pattern. In order to demonstrate the consistency of the kriging, a control map was provided for comparison, which was obtained directly with a more accurate (longer acquisition time of 280 s) AFI sequence with the same resolution than the kriged maps ($32 \times 32 \times 44$ resolution). The difference in the flask neck area (top left of K and MA maps) could be caused by some susceptibility artefact sensitive to the AFI sequence parameters, which could not be set exactly identical in the low and high resolution acquisitions.

DISCUSSION The kriging process does provide a fast and effective way to improve the quality of B_1^- maps without any enhanced SAR exposure. In addition to the experimental proof, kriging has also been tested with an inhomogeneous phantom composed of 8 human tissues in Finite Elements Method based simulations (Aarkid head model with Ansoft HFSS code). In this case, kriging provided even better results since the physical phase of B_1^- is given by the simulation. In the scope of this preliminary study, all the properties of the RF coil were not used to their full extent, especially the very different field distribution in the longitudinal and transverse directions. Two variograms could have been built from the measured maps for the kriging process to improve its performances. Some information about the nature of the AFI sequence noise or artefact could be extracted as well from the analysis of residual error between measured and kriged data. Finally, the entire kriging algorithm can be implemented on a personal computer and run in a 5-minute lasting routine.

REFERENCES [1] V. L. Yarnykh, Actual Flip-Angle Imaging in the Pulsed Steady State, Magn Reson Med 2007; 57:192-200. [2] H. Wackernagel, Multivariate Geostatistics - An Introduction with Applications, Springer 2003.

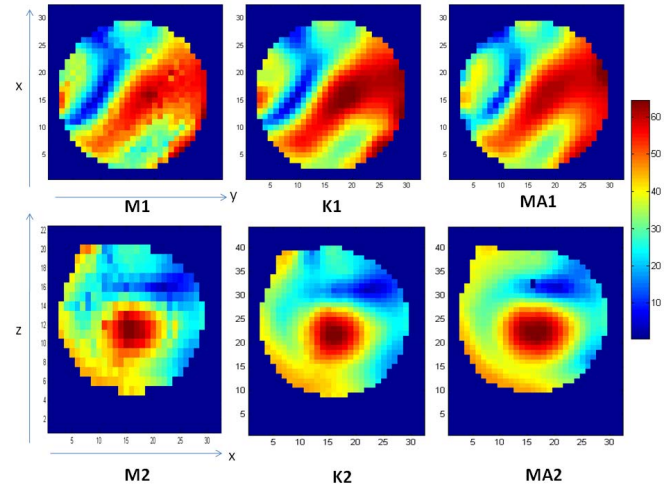


Fig. 1: Axial and sagittal flip angle maps: (1) $M1$, $M2$ show an interference obtained with low resolution B_1^- maps, measured channel by channel, (2) $K1$, $K2$ show the same interference obtained with kriged B_1^- maps, (3) $MA1$, $MA2$: show the same control interference obtained with combined channels measured directly at the kriging resolution.